

Three-dimensional data of wire-cut surface scans under the confocal microscope (110 character maximum, inc. spaces)

Yuhang Lin^{1,2,*}, Heike Hofmann^{2,3}, Curtis Mosher⁴, Eden Amin⁵, Jeff Salyards², and Alicia Carriquiry^{1,2}

¹Iowa State University, Department of Statistics, Ames, IA, 50011, USA

²Iowa State University, Center for Statistics and Applications in Forensic Evidence, Ames, IA, 50011, USA

³University of Nebraska-Lincoln, Department of Statistics, Lincoln, NE, 68583, USA

⁴Iowa State University, Roy J Carver High Resolution Microscopy Facility, Ames, IA, 50011, USA

⁵University of Central Oklahoma, Forensic Science Institute, Edmond, OK, 73034, USA

*corresponding author(s): Yuhang Lin (yhlin@iastate.edu)

ABSTRACT

Update later: max of 170 words: describe the study, the assay(s) performed, resulting data, and reuse potential

Wire cut data is important in forensic investigations but lacks a systematic way of analyzing the data. We created a data set of 120 scans of aluminum wire cut in $\times 3\mu$ format, using 5 wire cutters and 3 locations along the 4 blades, with 2 replicates for each combination. A systematic pipeline with multiple analysis plots was developed to analyze the data and draw conclusions based on numerical measures.

Background & Summary

An important part of a forensic analysis is the investigation of marks left at a crime scene. Forensic examiners are in particular interested in the origin of those marks, ie. in the investigation of their source. This is known as the Source Identification Problem in Forensic Science [citation?](#). The forensic science community generally distinguishes between the **specific source problem**, where the examiner is interested in whether a mark was left by a specific tool, and the **common source problem**, where the focus of the investigation is on whether two marks were left by the same tool. Current accepted practice in both of these situations is based on a visual inspection of the items under a comparison microscope and results, according to the Theory of Identification¹ developed by the Association of Firearm and Toolmark Examiners (AFTE), in a conclusion of the form *identification* (the marks are believed to have been made by the same source), *elimination* (the marks on the two items are believed to have been made by different tools), and *inconclusive* (there are not enough similarities or dissimilarities between the marks to allow either an identification or an elimination). At its core, this assessment is subjective in its nature and has been criticized in reports by the National Research Council² and the President's Council of Advisors on Science and Technology³ for its lack of objectivity and the absence of error rates.

Both of these issues rely on data with known ground-truth.

Biedermann⁴ distinguishes between internal and external perspectives in the forensic literature. The external perspective only allows general statements based on (black-box) studies relating examiners' conclusions to ground truth without considering any evidence of a particular case. To allow an internal perspective, there is a need to quantitatively capture the basis for an evaluation based on specific evidence.

When a bladed tool cuts a wire, striation marks are left on the cut surface of the wire, as shown in Figure 1.

Wire cut data is a type of forensic tool mark data used to assess similarity of striations left on the surface by a wire cutter. There have been cases where the evidence and testimony on wire cut evidence played a crucial role in the criminal investigation and conviction of a defendant.

However, there is a lack of a standardized method to analyze it, except for visual comparison.

Work on striations made by screwdrivers⁵ identified angle of attack⁶, rotational axis⁷, and direction⁸ as the main factors for comparisons.

Earlier research by Ma et al.⁹ and Zheng et al.¹⁰ has focused on collecting and distributing datasets for this purpose and providing a foundation for future advancements in tool mark analysis. Studies such as those by Chu et al.¹¹ and Vorburger et al.¹² have demonstrated the efficacy of using numerical methods to improve accuracy and consistency in tool mark analysis.



Figure 1. Microscopic close-up of striations left by a blade on the cut end of a wire.

42 Hare et al.¹³ and Ju et al.¹⁴ have explored methods for quantifying the similarity between representative signals, but alignment
43 remains a major hurdle.

44 In this study, we follow the same path and provide a data set of wire cut scans, and also discuss a systematic pipeline to
45 analyze the data and draw conclusions based on numerical measures. Here, we provide a data set containing multiple files, as
46 described in Table 1.

47 For the reproducibility of all our data and alignment results, we introduce in detail in [Cutting Wires](#) [hyperlink location](#)
48 [incorrect for unnumbered sections](#) it seems that the hyperlinks make sure that the section is on the page how we cut the wire
49 and collect the 120 scans with 5 tools, in [Extract Profiles](#) how we extract profiles from the scans, in [Filtered Signals](#) how we
50 filter signals from the profiles, in [Align Signals](#) how we align signals from different scans and optimize the alignment with the
51 cross-correlation function (CCF) values. In [Data Records](#), we discuss where our data is held. Then, in [Technical Validation](#),
52 a technical validation was conducted to further compare signals from different sources also match our assumption, together
53 with visual aids for drawing conclusions. Finally, in [Usage Notes](#), we provide available codes for creating the data set and
54 conducting technical validation, as discussed in [Methods](#) and [Technical Validation](#). [Code availability](#) discusses where these
55 codes are available online. We hope this pipeline developed using this data set to be further generalized and applied to real
56 crime scenes to help investigators draw conclusions based on real wire cut data.

57 **Methods**

58 In this study, we use aluminium wire [more details: thickness, brand?](#) to create cuts. The physical property of aluminum wire
59 makes it an excellent candidate for keeping marks while being relatively easy to bend and non-toxic, i.e. with a hardness of
60 XXX aluminium is soft enough that tools leave marks, but hard enough to not be affected by handling cut materials under the
61 microscope.

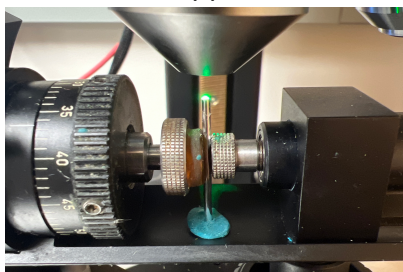
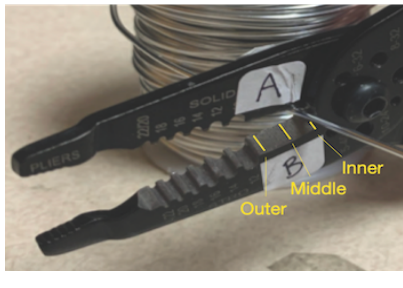
62 [XXX look up the hardness value of aluminium, copper and lead.](#) In real casework, aluminium wires are not seen as often
63 as lead or copper. We avoided using lead in the laboratory setting, because of its toxicity.

64 **Cutting Wires**

65 The aluminum wire used was 16 Gauge/1.5 mm, anodized. In order to cut the wire, 4-inch pieces were unspooled and cut
66 using Kaiweets wire cutters, model KWS-105, as shown in Figure 2a, for 1 blade location, either inner, middle, or outer, which
67 gives us 1 replicate. Each piece was then cut into half to create 2-inch pieces for each side, AB and CD, with a sharpie line
68 marking the cut ends, giving us 4 samples. Then, we use the standard scanning protocols for the confocal microscope, shown
69 in Figure Figure 2b, to scan the wire tip surfaces. The scanned surfaces are saved in a resolution of $0.645\mu\text{m} \times 0.645\mu\text{m}$ per
70 square pixel in an $\times 3\mu\text{m}$ file format. Here, we are showing AB and CD sides in Figure 2c, with the back of A being C and
71 the back of B being D. Both AB and CD sides form tent structures on the tips of the wire, and we separate each side of the
72 tent into 2 pieces along the bending position, resulting in 8 scans. We repeated this process for all 3 locations along the blade

Table 1. Structure of available data and files.

	Description	Section
Raw data		
scans/	folder containing 120 topographic 3d scans corresponding to 30 aluminum wire cuts (x3p format)	Cutting Wires
meta.csv	meta information for each cut with tool, blade, and location information (CSV format)	Cutting Wires
Manual derivatives		
profiles/	folder of files with manually extracted profiles (CSV format)	Extract Profiles
Computational derivatives in folder 'data-derived/'		
wire-signals	signals processed from corresponding profile (zipped CSV format)	Filtered Signals
wire_pairwise_ccf	CCF values of all pairwise aligned signals (zipped CSV format)	Align Signals
Image files		
pngs/	folder containing pictures of 3d scans of wire cuts (PNG format)	Cutting Wires
profile-images/	folder containing pictures of profile extracted from wire cuts (PNG format)	Extract Profiles
Visual Inventory in folder 'assessment/analysis-manual/'		
processing-wires	display of pairwise aligned signals from the same sources (HTML format)	Align Signals



(a)

(b)

Blade A

Blade C



Blade B

Blade D

(c)

Figure 2. (a) A Kaiweets wire cutter of model KWS-105 was used to cut the wire, with inner, middle and outer locations marked. (b) A confocal microscope was used to scan the wire surfaces. (c) After separating 2 tent structures by the connecting position, we obtained 4 samples - 2 samples from blade A and B, and others from blade C and D. width and height are tuned manually | full requirements see <https://www.nature.com/sdata/publish/submission-guidelines#figures>

and 5 wire cutters, with 2 replicates for each tool-edge-location combination, resulting in 120 scans. Each piece was labeled with the naming conventions, T(ool) 1/2/3/4/5 (Edge) A/B/C/D W(ire) - L(ocation) I(nner)/M(iddle)/O(uter) - R(epetition) 1/2, with T1AW-LI-R1 being the piece cut by tool 1 on the A edge at the inner location for the first repetition.

Extract Profiles

Numerical comparisons between 2 replicates cannot be done directly on the $\times 3p$ files. We need to extract representative functions from the scans first. A representative function with the most information is considered as a signal for one scan, which is used later for comparison. To obtain this function, we first need a profile of the scan, which is a sequence of values along a user-drawn line on the surface. The profile captures most features of the scan and be orthogonal to the striation marks of the scan, which are formed by the ups and downs of grooves. So, we draw the line across the wide region of the scan to maximize the feature captured, as shown in dark blue in Figure 3a. We then investigate the values under this profile line. The profile function along the line is plotted in Figure 3b.

Filtered Signals

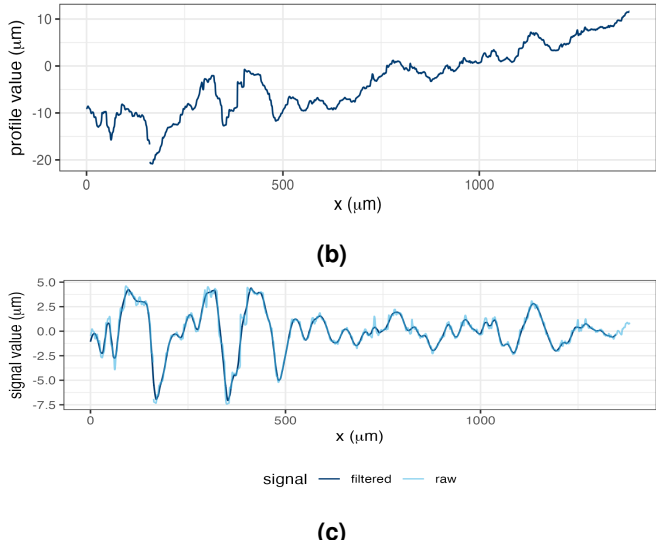
With the profile extracted, we then obtain the signal. Two Gaussian filters, as discussed in Cleveland et al.¹⁵, are applied to these resulting profiles. In particular, we first used a large low-pass filter with bandwidths of 400 microns to remove the large trend, as it overwhelms the signals, and then used a small high-pass filter of 40 microns to average across noise and remove spikes, as shown in Figure 3c. (add reference: W. S. Cleveland, E. Grosse and W. M. Shyu (1992) Local regression models. Chapter 8 of Statistical Models in S eds J.M. Chambers and T.J. Hastie, Wadsworth & Brooks/Cole.). Finally, the extreme tail values are removed.

Align Signals

Signals extracted from different scans are put together for comparison, and we maximize the cross-correlation function (CCF) values between the signals to find the best alignment numerically. For example, we compare T1AW-LI-R1 to T1AW-LI-R2, T1CW-LI-R1 to T1CW-LI-R2, and so on. That is comparing each row in Figure 4. We know that signals from two replicates with the same tool-edge-location combination yield similar signals as in the first and second columns of Figure 5, which results in alignments of massive overlapping and high CCF values close to 1. The alignments and values we got in the rightmost column of Figure 5 fulfill our expectations.



(a)



(b)

(c)

Figure 3. (a) A profile line in dark blue was drawn across the striations of the scan. (b) The profile function extracted along the profile line in (a). (c) The raw signal in light blue is obtained by using the low-pass filter on the profile function in (b) and the filtered signal is obtained by using the high-pass filter on the raw signal.

98 Data Records

99 The complete data set is available on the ISU DataShare repository at <https://iastate.figshare.com/>, which is public and open
100 access for every interested researcher. The structure of the data set is described before in Table 1.

101 Technical Validation

102 For the data collection process, two team members did the cutting and labeling together, then one person did the scanning and
103 named according to the naming convention introduced in [Cutting Wires](#). The scanning was done in a specific order to ensure
104 consistency across all scans. The data was saved in a consistent format to ensure easy of access for analysis. A third person
105 then checked the data to ensure that the data was consistent in naming and accurate.

106 For the validation of the scans and their processing, we investigate the correlation scores of pairwise aligned signals. Large
107 scores between signals are indicative of being made by the same tool. As shown previously in Figure 5 in [Align Signals](#), we
108 expect a high correlation score between signals from scans of wires cut with the same tool. For signals from scans of wires cut
109 with a different tool, we expect a low correlation score. For example, we have two scans from different tools, T1AW-LI-R1
110 and T2AW-LI-R1, as shown in Figure 6a and Figure 6b. The alignment is shown in Figure 6c with a 0.2 CCF value, which is
111 low, as expected.

112 We also put resulting CCFs for all pairwise comparisons in the boxplot, together with the receiver operating characteristic
113 (ROC) curve, as in Figure 7 and Figure 8. The CCF values for the same sources are close to 1, while the CCF values for
114 different sources are much lower than expected. This is consistent with our expectations and validates our data processing
115 pipeline.

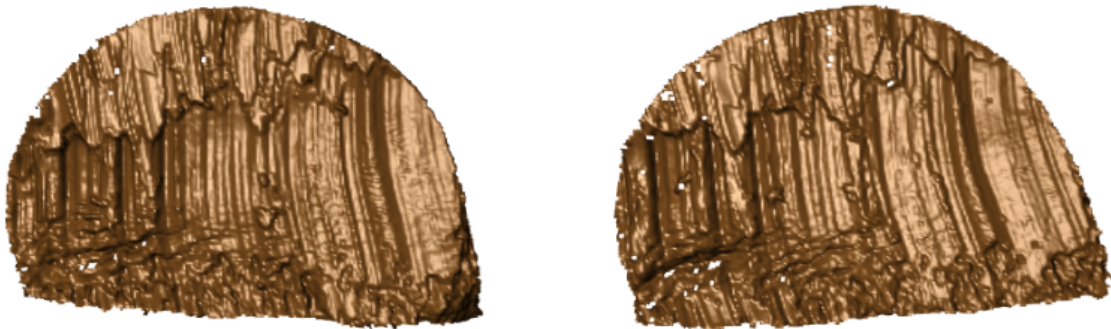
116 Usage Notes

117 The R package `x3ptools`¹⁶ available from CRAN supports working with files in `x3p` format. The sample scripts in R
118 for processing scans from `x3p` format to their signal and alignment are available on GitHub [heike/wirecuts-data](#) in the
119 assessment/code folder, as described in Table 2.

120 We already conduct pairwise comparisons and visualize some of the comparison results in [Align Signals](#) and [Technical
Validation](#), and other analysis plots as well.

122 Suppose we put the CCF values in a tilemap with different tools, locations and edge combinations. In that case, we expect
123 only the diagonal to have high CCF values, close to 1 and marked as orange in the tilemap, as the diagonal represents the
124 same source, and the rest of the matrix to have low CCF values, close to 0 and marked as gray. In Figure 9, the behavior is
125 consistent with our expectation overall, except for some rare cases with tool 5 edge D. The density plot in Figure 10 shows the

Edge A



Edge C



Edge B



Edge D



Figure 4. Scans from different sides of tool 1 at the inner location.

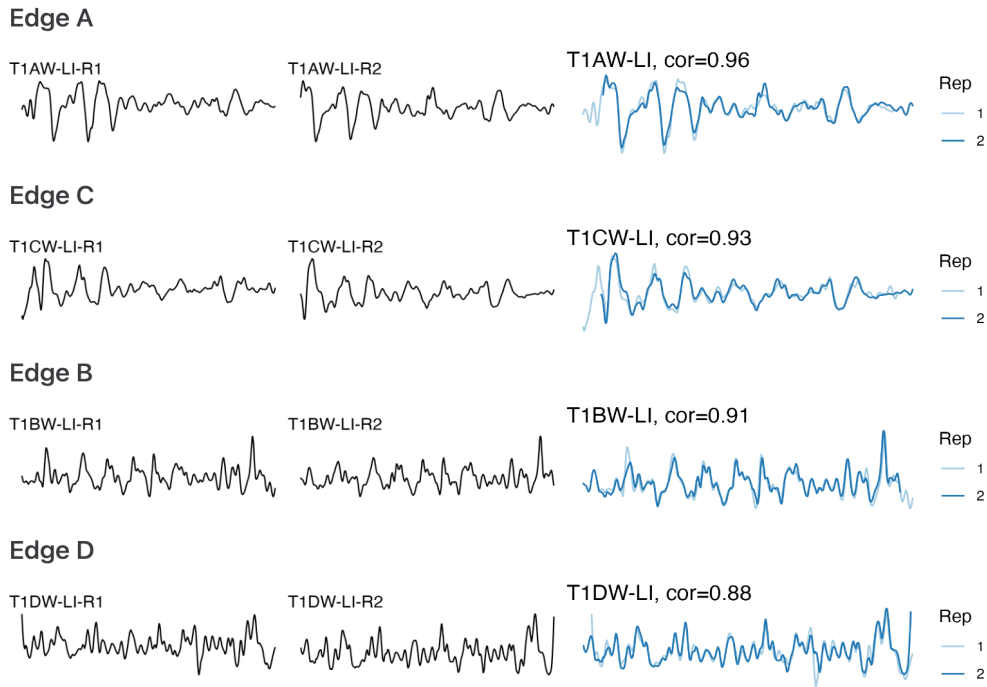


Figure 5. The first and second columns show the signals extracted from Figure 4, and the third column shows the alignments and CCF values between pairs of signals.

Table 2. Overview of available codes.

	Description	Section
Inspect raw scans		
1-create_pngs_from_x3p.R	obtain images of x3ps in scans /	Cutting Wires
Extract profiles		
2-create_profiles_from_x3p.R	manually extract profiles from each scan	Extract Profiles
3-create-single-profile-file.R	create meta profile information	Extract Profiles
Derive signals		
4-create_signals_from_profiles.R	derive signals from each profile	Filtered Signals
Align signals		
5-create-images.R	create images for pairwise alignment	Align Signals
6-align-pairwise.R	compute pairwise alignment CCF values	Align Signals
7-all-comparison-results.R	visualize comparison results	Align Signals

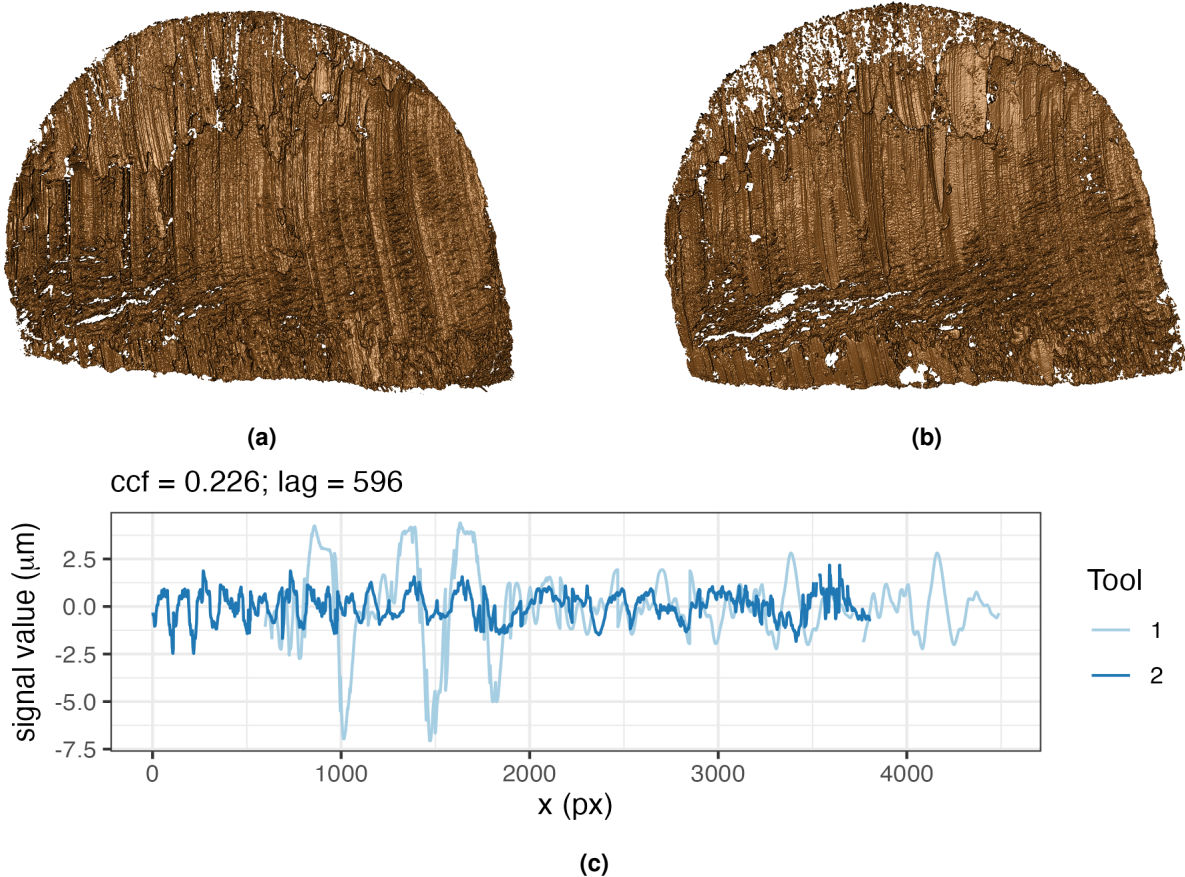


Figure 6. (a) Scan T1AW-LI-R1 cut by tool 1. (b) Scan T2AW-LI-R1 cut by tool 2. (c) Alignment of signals from T1AW-LI-R1 and T2AW-LI-R1.

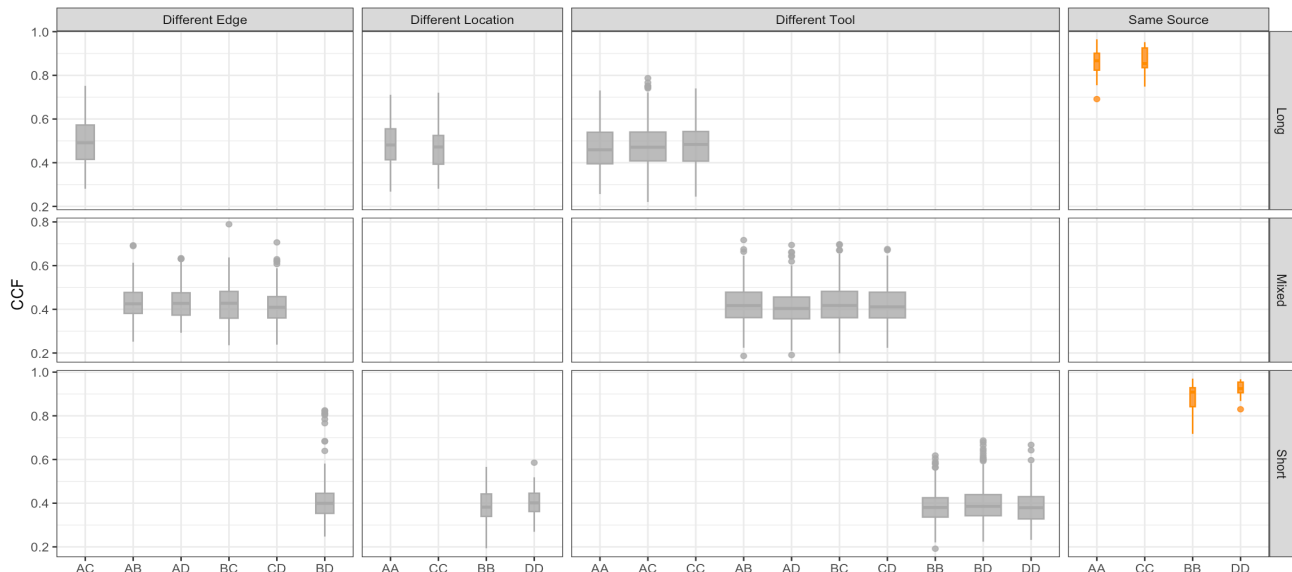


Figure 7. The boxplot shows that signals from the same sources have higher CCFs than those from different sources.

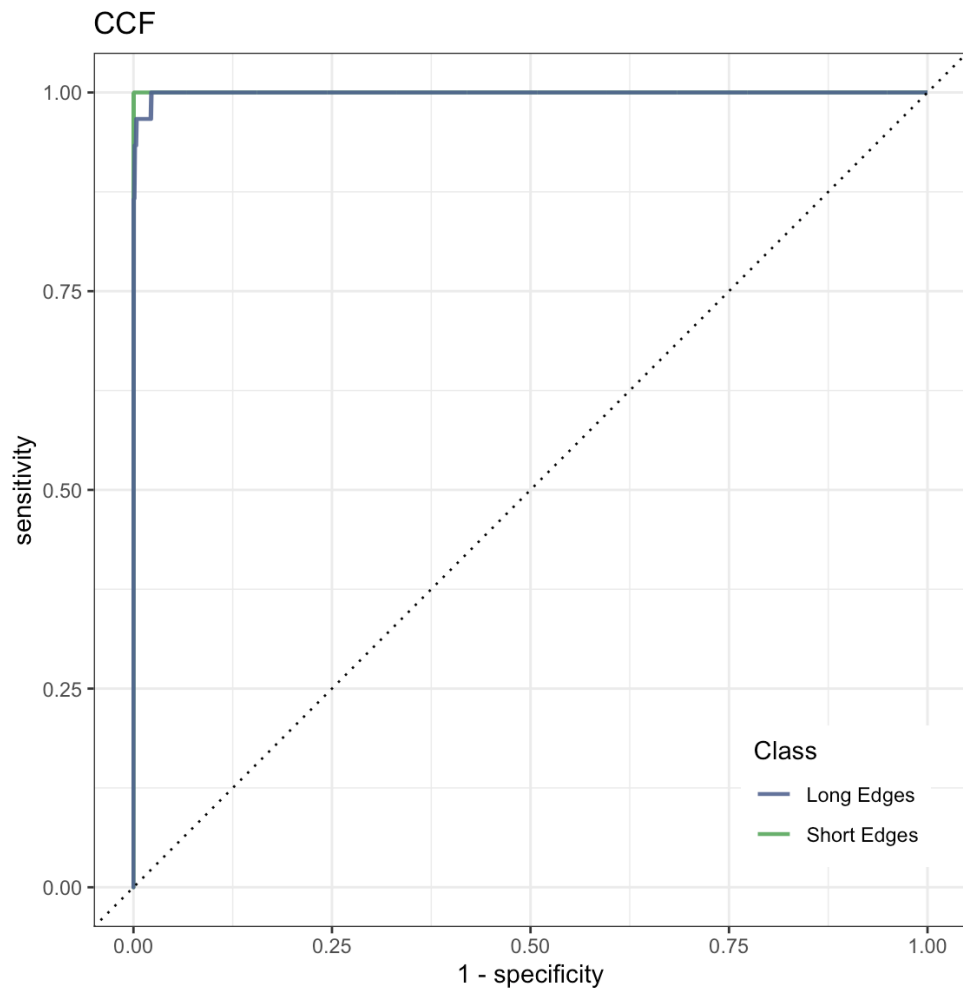


Figure 8. The ROC curve is bending very close to the upper left corner, which means excellent in classification and drawing conclusions.

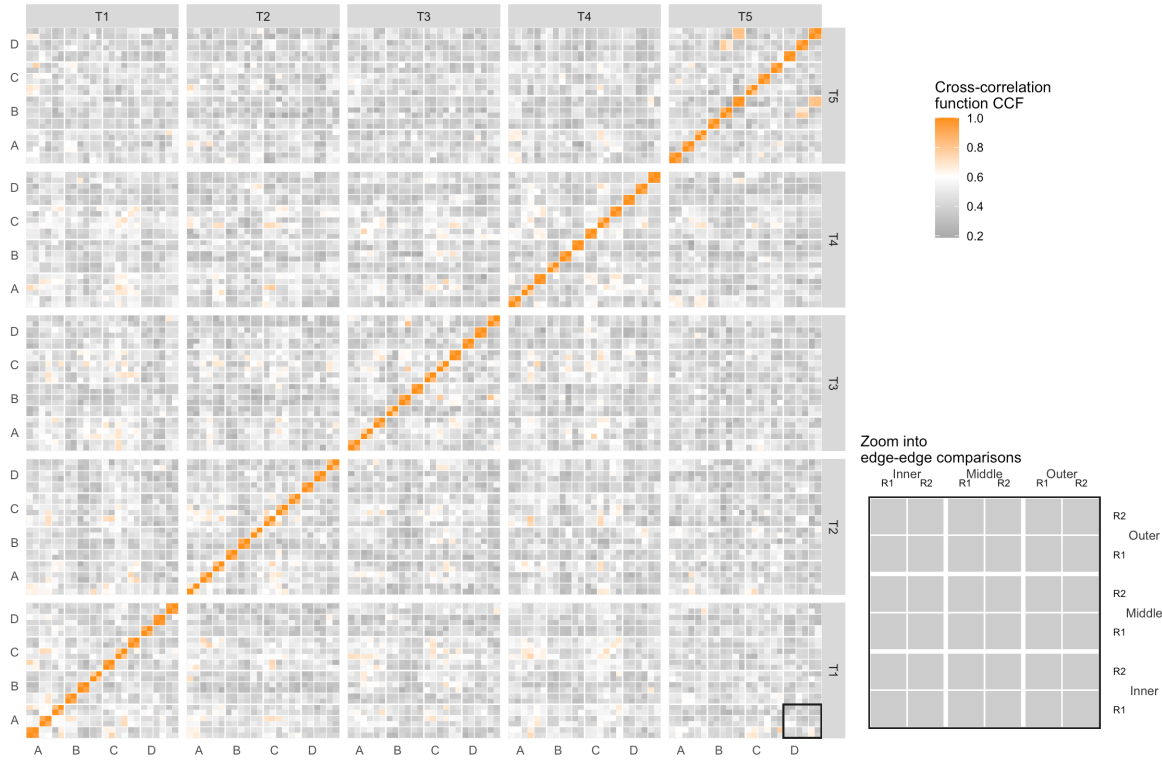


Figure 9. The tilemap shows signals from the same source have CCFs close to 1.

126 distribution of the CCF values with the same sources and different sources. The overlapping points between the tails of these
 127 two distributions to be a rough threshold.

128 Furthermore, the ROC curve in Figure 8 shows the sensitivity / true positive rate against the false positive rate (FPR) (1 -
 129 specificity). The curve is very close to the upper left corner, which is excellent for classification and drawing conclusions. It
 130 gives us a true threshold of 0.589 to control the FPR to be less than 0.05 with a false negative rate (FNR) to be 0, (false positive
 131 rate (FPR) / false discovery rate (FDR) -> define the H0 or call it false identification rate (FIR)???, and 0.658 to control the
 132 FPR to be less than 0.01, with FNR to be 0.02.

133 **Code availability**

134 We made available all codes we used for inspecting raw scans, extracting profiles, deriving signals, aligning signals, and visualizing
 135 comparison results discussed in [Methods](#) and [Technical Validation](#), as described in Table 2. All results are reproducible
 136 using these codes provided.

137 **References**

- 138 1. AFTE. The association of firearm and tool mark examiners: Theory of identification as it relates to toolmarks. *AFTE J.* **30**, 86–88 (1998).
- 139
- 140 2. NRC. *National Research Council: Strengthening Forensic Science in the United States: A Path Forward* (National
 Academies Press, 2009).
- 141
- 142 3. President's Council of Advisors on Science and Technology. *President's Council of Advisors on Science and Technology: Forensic Science in Criminal Courts: Ensuring Scientific Validity of Feature-Comparison Methods* (Executive Office of
 the President of the United States, President's Council, Washington, D.C., 2016).
- 143
- 144
- 145 4. Biedermann, A. The strange persistence of (source) “identification” claims in forensic literature through descriptivism,
 diagnosticism and machinism. *Forensic Sci. Int. Synerg.* **4**, 100222, [10.1016/j.fsisyn.2022.100222](https://doi.org/10.1016/j.fsisyn.2022.100222) (2022).
- 146

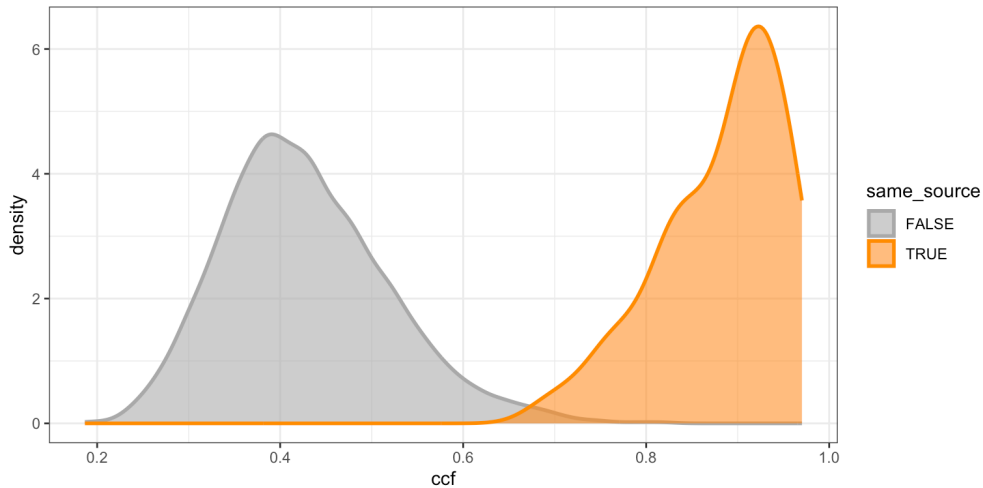


Figure 10. The density plot shows tails of distributions overlap, which to be used as a rough threshold for drawing conclusions.

- 147 5. Baiker, M. *et al.* Quantitative comparison of striated toolmarks. *Forensic Sci. Int.* **242**, 186–199, [10.1016/j.forsciint.2014.06.038](https://doi.org/10.1016/j.forsciint.2014.06.038) (2014).
- 148
- 149 6. Baiker, M., Pieterman, R. & Zoon, P. Toolmark variability and quality depending on the fundamental parameters: Angle
150 of attack, toolmark depth and substrate material. *Forensic Sci. Int.* **251**, 40–49, [10.1016/j.forsciint.2015.03.003](https://doi.org/10.1016/j.forsciint.2015.03.003) (2015).
- 151
- 152 7. Garcia, D. L., Pieterman, R. & Baiker, M. Influence of the axial rotation angle on tool mark striations. *Forensic Sci. Int.*
153 **279**, 203–218, [10.1016/j.forsciint.2017.08.021](https://doi.org/10.1016/j.forsciint.2017.08.021) (2017).
- 154
- 155 8. Cuellar, M., Gao, S. & Hofmann, H. An algorithm for forensic toolmark comparisons. *Forensic Sci. Int. Synerg.* **9**,
156 100543, [10.1016/j.fsisyn.2024.100543](https://doi.org/10.1016/j.fsisyn.2024.100543) (2024).
- 157
- 158 9. Ma, L. *et al.* NIST Bullet Signature Measurement System for RM (Reference Material) 8240 Standard Bullets. *J. Forensic
159 Sci.* **49**, 1–11, [10.1520/JFS2003384](https://doi.org/10.1520/JFS2003384) (2004).
- 160
- 161 10. Zheng, X. A., Soons, J. A. & Thompson, R. M. NIST Ballistics Toolmark Research Database | NIST (2016).
- 162
- 163 11. Chu, W., Thompson, R. M., Song, J. & Vorburger, T. V. Automatic identification of bullet signatures based on consecutive
164 matching striae (CMS) criteria. *Forensic Sci. Int.* **231**, 137–141, [10/gn65cz](https://doi.org/10/gn65cz) (2013).
- 165
- 166 12. Vorburger, T. *et al.* Applications of cross-correlation functions. *Wear* **271**, 529–533, [10.1016/j.wear.2010.03.030](https://doi.org/10.1016/j.wear.2010.03.030) (2011).
- 167
- 168 13. Hare, E., Hofmann, H., Carriquiry, A. *et al.* Automatic matching of bullet land impressions. *The Annals Appl. Stat.* **11**,
2332–2356, [10.1214/17-AOAS1080](https://doi.org/10.1214/17-AOAS1080) (2017).
- 169
- 170 14. Ju, W. & Hofmann, H. The R Journal: An Open-Source Implementation of the CMPS Algorithm for Assessing Similarity
171 of Bullets. *The R J.* **14**, 267–285, [10.32614/RJ-2022-035](https://doi.org/10.32614/RJ-2022-035) (2022).
- 172
- 173 15. Cleveland, W. S., Grosse, E. & Shyu, W. M. Local Regression Models. In *Statistical Models in S* (Routledge, 1992).
- 174
- 175 16. Hofmann, H., Vanderplas, S., Krishnan, G. & Hare, E. X3ptools: Tools for Working with 3D Surface Measurements,
176 [10.32614/CRA.N.package.x3ptools](https://doi.org/10.32614/CRA.N.package.x3ptools) (2018).

168 Acknowledgements

169 This work was partially funded by the Center for Statistics and Applications in Forensic Evidence (CSAFE) through Cooper-
170 ative Agreement 70NANB20H019 between NIST and Iowa State University, which includes activities carried out at Carnegie
171 Mellon University, Duke University, University of California Irvine, University of Virginia, West Virginia University, Univer-
172 sity of Pennsylvania, Swarthmore College and the University of Nebraska-Lincoln.

173 **Author contributions statement**

174 Let's follow the Elsevier definitions: <https://www.elsevier.com/researcher/author/policies-and-guidelines/credit-author-statement>
175 Y.L.: Methodology, Software, Validation, Data Curation, Writing - Draft; H.H.: Conceptualization, Methodology, Valida-
176 tion, Writing - Review & Editing; C.M.: Lab supervision; E.A.: Physical Specimen, Scanning; J.S: Forensic advice; A.C.:
177 Funding acquisition.
178 All authors reviewed the manuscript.

179 **Competing interests**

180 (mandatory statement)
181 H.H. is a technical advisor to AFTE (Association of Firearms and Toolmarks Examiners), fellow of the ASA (American
182 Statistical Association), and committee member of the ASA Forensic Science Committee. H.H. has testified as court witness
183 on behalf of judge April Neubauer, NY State Supreme Court Criminal Term in New York City. [other competing interests -](#)
184 [Alicia?](#)